Inelastic longitudinal electron scattering C2 form factors in ^{60}Ni

Firas Z. Majeed[1] and Fadhel M. Hmood*[1]

1Department of physics, College of Science, Baghdad University, Baghdad, Iraq.
* Corresponding Author: hmoodfadhel@gmail.com

Abstract: Inelastic longitudinal C2 form factors in 60Ni nucleus have been studied using the nuclear shell model that carried out in terms of configuration mixing with limiting number of orbits in the model-space (restricted model space) (2p3/2, 2p1/2,1f5/2)n and including the effects of the discarded space (core orbits + higher orbits) outside the model-space, which is called core-polarization effects, through a microscopic theory as first-order perturbation theory that considers particle-hole excitations from the core orbits and via the model-space orbits into the higher orbits with 2ħ excitations. The shell-model wave functions obtained with the configuration, with a number of active neutrons outside the inert core 56Ni. The effective interaction F5PVH potential is used to generate the model space wave function. The simple harmonic oscillator (HO) potential is used to generate the single particle wave functions. Two realistic interactions had been adopted as a residual interactions to couple the particle-hole pair represented by the two body Michigan sum of three range Yukawa potential (M3Y-P2) and Gogny. The obtained theoretical results had been compared with available experimental data.

Keyword: core polarization, 60Ni, form factor.

Introduction

Electron scattering is an excellent tool for studying the nuclear structure because of many reasons. Since the interaction between the electron and the target nucleus is relatively weak of order α =1/137, the fine-structure constant, and known where the electron interacts electromagnetically with the local charge, current and magnetization densities of nucleus. [1].

A perfect and good information about the nuclear structure can be obtained from the electron scattering by the nucleus at high energy. When the energy of the incident electron is in the range of 100 MeV and more, the de Broglie wavelength will be in the range of the spatial extension of the target nucleus, Thus with these energies, the electron represents a best probe to study the nuclear structure [2][3].

The electrons scattering from a target nucleus can occur in two types: first, the nucleus is left in its ground state after the scattering and the energy of the electrons is unchanged, this processes is called "Elastic Electron Scattering". In the second the scattered electron leaves the nucleus in different excited state which has a final energy reduced from the initial just by the amount taken up by the nucleus in its excited state, this processes is called " Inelastic Electron Scattering" [4][5].

It is known that the inelastic electron scattering has proven to be a good technique for studying the properties of excited states of nuclei, in particular their spins, parities, and the strength and structure of the transition operators connecting the ground and the excited states.[6].

The form factor can be found experimentally as a function of the momentum transfer (q) by knowing the energies of the incident and scattered electron and the scattering angle.

Using the experiment to study the inelastic scattering of electrons from 60Ni with an over-all energy resolution of 0.1% by the use of 183 MeV and 250 MeV electron beams from the Tohoku 300 MeV linear accelerator [11].

The electron scattering process can be explained according to the first Born approximation as an exchange of a virtual photon carrying a momentum between the electron and nucleus. The first Born approximation is being valid only if $Z\alpha<<1$, where α is the fine structure constant [7].

The scattering cross section for relativistic electrons from spinless nucleus of charge Ze, where Z is the number of protons in the nucleus, was first derived by Mott (1929) [8].

The nickel isotopes had been described in terms of strongly admixed spherical shell-model configurations of neutrons occupying the 2p3/2, 1f5/2, and 2p1/2 orbits. A set of effective-interaction matrix elements is deduced which accurately reproduces the spectra of the Ni isotopes from Ni58 to Ni67. The wave functions resulting from the calculations of the energy levels are then used to calculate the single-nucleon spectroscopic factors. These are in fairly good agreement with the experimental spectroscopic factors found in pickup and stripping experiments. the E2 transition probabilities in the even-mass isotopes of Ni are calculated and found to be in agreement with experimental facts [9].

A report of experimental for a set of inelastic form-factor measurements on the first excited state of 58Ni, 60Ni, and 62Ni, which, together with the accurate Coulomb-excitation B(E2) measurements by Stelson and McGowan, provide for the first time an accurate experimental check on the distorted-wave calculation of Griffy et al. The experimental measurements were carried out at the Yale Linear Electron Accelerator Laboratory using incident energies ranging from 45 to 65 MeV and scattering angles from 70 to 130° [10].

Inelastic electron scattering cross sections have been measured up to a momentum transfer q=3.9 fm-1, determining very precisely the transition charge density of the first excited (2+1) state of 58Ni. The results have been

interpreted in a fully self-consistent theoretical treatment for both the ground state and the (2+1) transition charge density of 58Ni [12].

Elastic and inelastic electron-scattering form factors for multipolarities up to t = 7 and some transition-strength distributions are calculated with shell-model wave functions for about ten target nuclei in the mass range A = 52-62 including 52,53Cr, 54,56Fe, 53Cr, 55Mn, 59Co and 58,60,62Ni. It is found that the strengths of the calculated magnetic transitions are always less than about 50% of the pure single-particle values [13].

A microscopic description of data on the inelastic scattering for factors for the $0^+ \rightarrow 2^+$ as well as $0^+ \rightarrow 4^+$ transitions in some doubly even Ti, Cr, Fe, Zn, and Ni isotopes including 58,60,62Ni is attempted in terms of the projected Hartree-Fock-Bogoliubov wave functions resulting from realistic effective interactions operating in the 2p-1f shell [14].

The effective interaction GXPF1 for shell-model calculations in the full pf shell had been tested in detail from various viewpoints such as binding energies, electromagnetic moments and transitions, and excitation spectra. The semi magic structure is successfully described for N or Z=28 nuclei, 53Mn, 54Fe, 55Co, and 56,57,58,59Ni, suggesting the existence of significant core excitations in low-lying model over conventional calculations in cases where full-space calculations still remain too large to be practical [15].

The experimental single-particle energies and occupation probabilities for neutron states near the Fermi energy in 58,60,62,64 Ni nuclei had studied and obtained from joint evaluation of the data on nucleon stripping and pickup reactions on the same nucleus. The resulting data had been analyzed within a mean_field model with dispersive optical_model potential. Good agreement had been obtained between the calculated and experimental [16] .

High-precision reduced electric-quadrupole transition probabilities B(E2; 0+1→ 2+1) have been measured from single-step Coulomb excitation of semi-magic 58,60,62,64Ni (Z = 28) beams at 1.8 MeV per nucleon on a natural carbon target. The energy loss of the nickel beams through the carbon target were directly measured with a zero-degree Bragg detector and the absolute B(E2) values were normalized by Rutherford scattering. The B(E2) values disagree with recent lifetime studies that employed the Doppler-shift attenuation method [17].

Calculated elastic and inelastic form factors and for the transition from the ground state to J+1 (L = J = 2, 4) state in 58−68Ni and 24Mg, carried out the starting point of the method were a set of Hartree-Fock-Bogoliubov wave functions generated with a constraint on the axial quadrupole moment and using a Skyrme energy density functional [18].

The Core Polarization (CP) effects derivation with higher configuration in the first order perturbation theory and the two-body matrix elements of three parts of realistic interaction: central, spin orbit and tensor force which are belong to M3Y-P2 and Gogny as a residual interactions in a separate pictures will be studied in the present work

A computer program is written in FORTRAN 90 language to include realistic interaction M3Y and Gogny in the original code which is written by Prof. Dr. R.A.Radhi, which then modified by assistance Prof. Dr. Firas Zuhair Majeed to receive new terms and fitting parameters [19].

Theory

Many particle matrix elements of the electron scattering operator $\hat{T}^{\eta}_{\Lambda}$ are expressed as the sum of the product of the one-body density matrix elements (OBDM) times the single-particle transition matrix elements [20]:

$$\left\langle \Gamma_f \left\| \hat{T}^{\eta}_{\Lambda} \right\| \Gamma_i \right\rangle = \sum_{\alpha,\beta} OBDM\left(\Gamma_i,\Gamma_f,\alpha,\beta\right) \left\langle \alpha \left\| \hat{T}^{\eta}_{\Lambda} \right\| \beta \right\rangle \quad (1)$$

where $\Lambda = JT$ is the multi-polarity in spin and isospin respectively, and the states $\Gamma_i \equiv J_i T_i$ and $\Gamma_f \equiv J_f T_f$ are the initial and final states of the nucleus, while α and β denote the final and initial single-particle states, respectively (isospin is included). The reduced matrix elements of the electron scattering operator $\hat{T}^{\eta}_{\Lambda}$ consist of two parts, one is the "Model space" matrix elements and the other is the "Core-polarization" matrix elements [21].

$$\left\langle \Gamma_f \left\| \hat{T}^{\eta}_{\Lambda} \right\| \Gamma_i \right\rangle = \left\langle \Gamma_f \left\| \hat{T}^{\eta}_{\Lambda} \right\| \Gamma_i \right\rangle_{MS} + \left\langle \Gamma_f \left\| \delta\hat{T}^{\eta}_{\Lambda} \right\| \Gamma_i \right\rangle_{CP} \quad (2)$$

$\left\langle \Gamma_f \left\| \hat{T}^{\eta}_{\Lambda} \right\| \Gamma_i \right\rangle_{MS}$ is the model-space matrix elements.

$\left\langle \Gamma_f \left\| \delta\hat{T}^{\eta}_{\Lambda} \right\| \Gamma_i \right\rangle_{CP}$ is the core-polarization matrix elements.

$\left|\Gamma_i\right\rangle$ and $\left|\Gamma_f\right\rangle$ are described by the model-space wave functions.

The model-space matrix elements are expressed as the sum of the product of the one-body density matrix elements (OBDM) times the single-particle matrix elements which are given by:

$$\left\langle \Gamma_f \left\| \hat{T}^{\eta}_{\Lambda} \right\| \Gamma_i \right\rangle_{MS} = \sum_{\alpha,\beta} OBDM\left(\Gamma_i,\Gamma_f,\alpha,\beta\right) \left\langle \alpha \left\| \hat{T}^{\eta}_{\Lambda} \right\| \beta \right\rangle_{MS} \quad (3)$$

The core-polarization matrix element in equation (2) can be written as follows [21]:

ISSN 2229-5518

$$\left\langle \Gamma_f \left\| \delta\hat{T}^{\eta}_{\Lambda} \right\| \Gamma_i \right\rangle_{cp} = \sum_{\alpha,\beta} OBDM(\Gamma_i,\Gamma_f,\alpha,\beta) \left\langle \alpha \left\| \delta\hat{T}^{\eta}_{\Lambda} \right\| \beta \right\rangle_{cp}$$

(4)

According to the first order perturbation theory, the single-particle matrix element for the higher-energy configurations is given by [22]:

$$\left\langle \alpha \left| \delta\hat{T}^{\eta}_{J} \right| \beta \right\rangle = \left\langle \alpha \left| \hat{T}^{\eta}_{J} \frac{Q}{E-H^{(0)}} V_{res} \right| \beta \right\rangle + \left\langle \alpha \left| V_{res} \frac{Q}{E-H^{(0)}} \hat{T}^{\eta}_{J} \right| \beta \right\rangle \quad (5)$$

where V_{res} is adopted here as a residual nucleon-nucleon interaction.

The single-particle energies are calculated according to [22]:

$$e_{nlj} = (2n+l-\frac{1}{2})\hbar\omega + \begin{cases} -\frac{1}{2}(l+1)\langle f(r)\rangle_{nl} & for\ j=l-\frac{1}{2} \\ \frac{1}{2}l\langle f(r)\rangle_{nl} & for\ j=l+\frac{1}{2} \end{cases} \quad (6)$$

with:

$$\langle f(r)\rangle_{nl} \approx -20A^{-2/3} MeV$$

$$\hbar\omega = 45A^{-1/3} - 25A^{-2/3} \quad (7)$$

The realistic M3Y and Gogny effective nucleon-nucleon interaction, which is used in electron scattering (Vres =v12) is expressed as a sum of the central potential part $v_{12}^{(C)}$, spin-orbit potential part $v_{12}^{(LS)}$, long range tensor part $v_{12}^{(TN)}$, and density dependence part $v_{12}^{(DD)}$ as follows [23]:

$$v_{12} = v_{12}^{(c)} + v_{12}^{(LS)} + v_{12}^{(TN)} + v_{12}^{(DD)} \quad (8)$$

The four potentials are expressed as [23]:

$$v_{12}^{(c)} = \sum_n (t_n^{(SE)} P_{SE} + t_n^{TE} P_{TE} + t_n^{(SO)} P_{SO} + t_n^{(TO)} P_{TO}) f_n^{(C)}(r_{12})$$

$$v_{12}^{(LS)} = \sum_n (t_n^{(LSE)} P_{TE} + t_n^{(LSO)} P_{TO}) f_n^{(LS)}(r_{12}) L_{12}.(\vec{s}_1 + \vec{s}_2)$$

$$v_{12}^{(TN)} = \sum_n (t_n^{(TNE)} P_{TE} + t_n^{(TNO)} P_{TO}) f_n^{(TN)}(r_{12}) r_{12}^2 S_{12}$$

$$v_{12}^{(DD)} = \left\{ t^{DD} P_{SE}.[\rho(r_1)]^{a^{(SE)}} + t^{DD} P_{TE}.[\rho(r_1)]^{a^{(TE)}} \right\} \delta(r_{12}) \quad (9)$$

where

$$f_n(r) = \frac{e^{-\mu_n r}}{\mu_n r}$$ for M3Y interaction, μ_n: range parameter

$$f_n^{C}(r) = e^{-(\mu_n r)^2}$$, $f_n^{LS} = \nabla^2\delta(r)$ represented Gogny interaction,

then for M3Y, eq. (9) becomes:

$$v_{12}^{(c)} = \sum_n (t_n^{(SE)} P_{SE} + t_n^{TE} P_{TE} + t_n^{(SO)} P_{SO} + t_n^{(TO)} P_{TO}) \frac{e^{-\mu_n r}}{\mu_n r}$$

$$v_{12}^{(LS)} = \sum_n (t_n^{(LSE)} P_{TE} + t_n^{(LSO)} P_{TO}) f_n^{(LS)}(r_{12}) L_{12}.(\vec{s}_1 + \vec{s}_2)$$

$$v_{12}^{(TN)} = \sum_n (t_n^{(TNE)} P_{TE} + t_n^{(TNO)} P_{TO}) f_n^{(TN)}(r_{12}) r_{12}^2 S_{12}$$

$$v_{12}^{(DD)} = \left\{ t^{DD} P_{SE}.[\rho(r_1)]^{a^{(SE)}} + t^{DD} P_{TE}.[\rho(r_1)]^{a^{(TE)}} \right\} \delta(r_{12}) \quad (10)$$

And for Gogny eq.(9) becomes:

$$v_{12}^{(c)} = \sum_n (t_n^{(SE)} P_{SE} + t_n^{TE} P_{TE} + t_n^{(SO)} P_{SO} + t_n^{(TO)} P_{TO}) e^{-(\mu_n r)^2}$$

$$v_{12}^{(LS)} = \sum_n (t_n^{(LSE)} P_{TE} + t_n^{(LSO)} P_{TO}) \nabla^2\delta(r) L_{12}.(\vec{s}_1 + \vec{s}_2)$$

$$v_{12}^{(TN)} = \sum_n (t_n^{(TNE)} P_{TE} + t_n^{(TNO)} P_{TO}) f_n^{(TN)}(r_{12}) r_{12}^2 S_{12}$$

$$v_{12}^{(DD)} = \left\{ t^{DD} P_{SE}.[\rho(r_1)]^{a^{(SE)}} + t^{DD} P_{TE}.[\rho(r_1)]^{a^{(TE)}} \right\} \delta(r_{12}) \quad (11)$$

where $t_n^{(SE)}$, $t_n^{(SO)}$, $t_n^{(TO)}$, $t_n^{(TE)}$ are the strength parameter in central part for (singlet-even), (singlet-odd), (triplet-odd) and (triplet-even), and $t_n^{(LSE)}$, $t_n^{(LSO)}$ are the strength parameter in the spin –orbit part for (singlet-even), (singlet-odd), $t_n^{(TNE)}$, $t_n^{(TNO)}$, are the strength parameter in tensor part for (tensor even), (tensor-odd) and tDD(SE) , tDD(TE) are the strength parameter in desity dependence parts for (single-even), (triplet-even) respectively. These parameter values are given in Table (1) [23].

Table (1). Shows the values of the best fit to the potential parameters for M3Y-P2 [23].

	R1=0.25 fm	R2=0.40 fm	R3=1.414 fm
Oscillator matrix elements (Channel)	t1	t2	t3
Centeral Singlet-Even (SE)	8027	-2880	-10.463
Central Triplet-Even (TE)	6080	2730	31.389
Central Singlet-Odd (SO)	-11900	-4266	-10.463
Central Triplet-Odd (TO)	3800	-780	3.488
Tensor-Even (TNE)	-131.52 MeV fm-2	-3.708 MeV fm-2	0.0
Tensor-Odd (TNO)	29.28 MeV fm-2	1.872 MeV fm-2	0.0
Spin-Orbit Even (LSE)	-9181.8	-606.6	0.0
Spin-Orbit Odd (LSO)	-3414.6	0.0	0.0
Desity- single even (SE)	181 MeV fm	0.0	0.0
Desity-Triplet even (TE)	1139 MeV fm	0.0	0.0

Results and Discussion

In this work, the model space adopted which is 2p3/2 1f5/2 2p1/2 configuration for 60Ni nucleus. Core-polarization effects are taken into account through first order perturbation theory, which allows particle-hole excitation from shell core orbits 1s1/2, 1p3/2, 1p1/2, 1d5/2, 2s1/2, 1d3/2 and 1f7/2 (shell model space having 56Ni as an inert core).

The effective interaction of model space F5PVH potential has been used to give the (1f5/22p3/22p1/2) shell model wave functions for 60Ni.

The single particle wave functions of the harmonic oscillator (HO) with size parameter b= 1.988 fm are used [24].

Two realistic interactions M3Y-P2 and Gogny as a residual interaction are used with the longitudinal C2 form factors of 60Ni from the ground state (JπT=0+2) to the excited state (JπT=2+2) at Ex=1.404 MeV have been calculated with core contribution only, since the model space neutrons has no contribute to the charge form factor, because they are neutral particles, then only core protons will be play this role.

Figure (1) using M3Y interaction as a residual interaction shows that an agreement is obtained for the first maximum (3×10-3) of the form factor for momentum transfer range 0≤q≤1.75fm-1, but the second maximum (1×10-5) of the form factor for the q range 1.75≤q≤3 fm-1 had been quenched, that is clear the calculations underestimate the experimental data for the first maximum, and overestimate for second maximum, there are a clear deviation in diffraction minimum from the theoretical calculations to the experimental data approximately 0.7 fm-1 with respect to the q values.

Figure (2) using Gogny interaction shows that the form factor value about 4x10-3 represented the first maximum for the range 0≤q≤1.75 fm-1, which is an agreement is obtained with experimental data up to q=1 fm-1, but the second maximum (5×10-6) for q range 1.75≤q≤3 fm-1 have been quenched, clearly the calculations underestimate the experimental data for the first maximum and overestimate for the second maximum,

The OBDM elements for this transition are shown in Table (2). The experimental data are taken from Ref. [18].

Table (2): Values of the OBDM elements for the longitudinal C2 transition of the 2_1^+ 2 , first state of 60Ni using F5PVH model space effective interaction for M3Y and Gogny at EX=1.404 MeV.

Ji	Jf	OBDM (ΔT=0)	OBDM (ΔT=1)
5/2	5/2	-0.41706	-0.29491
5/2	3/2	0.21388	0.15124
5/2	1/2	-0.34433	-0.24348
3/2	5/2	-0.14063	-0.09944
3/2	3/2	-0.68335	-0.48320
3/2	1/2	-0.34200	-0.24183
1/2	5/2	-0.37332	-0.26398
1/2	3/2	0.56073	0.39649

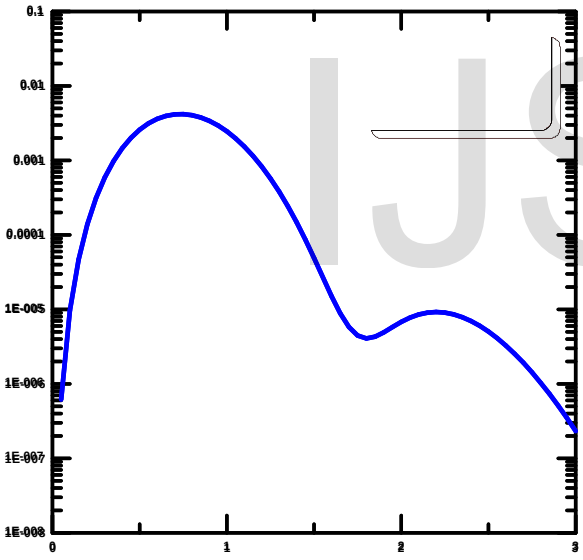

Fig. (1): Inelastic longitudinal C2 form factors for the 2_1^+2 state at Ex=1.404 MeV in ^{60}Ni with residual interaction M3Y (solid curve), the experimental data (filled circles) were taken from Ref. [18].

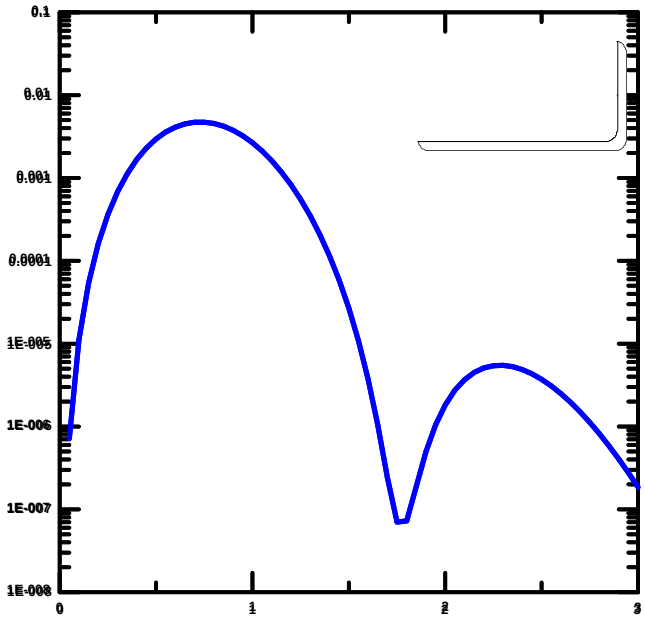

Fig. (2): Inelastic longitudinal C2 form factors for the 2_1^+2 state at Ex=1.404 MeV in ^{60}Ni with residual interaction Gogny (solid curve), the experimental data (filled circles) were taken from Ref.[18].

Figure (3) shows the quadrupole C2 form factor for the second transition from the ground state (JπT=0+2) to the final state (JπT=2+2) at Ex=2.151 MeV, with a residual interaction M3Y, only one lobe are obtained with form factor value equal to 2×10-3 for the momentum transfer range 0 ≤q≤3 fm-1, while the experimental data have two lobes, with form factor values equal to 1×10-3 for q range 0≤q≤1 fm-1, and 0.5×10-4 for q range 1≤q≤2 fm-1. The calculations results are not coincidence with the experimental data.

Figure (4), using Gogny as a residual interaction, only one lobe was obtained of form factor, which is equal to 0.5×10-3 with momentum transfer range 0 ≤q≤3 fm-1, and two lobes for experimental data, with the form factor value equal to 1×10-3 for q range 0≤q≤1 fm-1, and 0.5×10-4 for q range 1≤q≤2 fm-1. The calculations results are not coincidence with the experimental data.

The OBDM elements for this transitions are shown in Table (3). The experimental data are taken from Ref. [18].

Table (3): Values of the OBDM elements for the longitudinal C2 transition of the 2_2^+2, second state of 60Ni using F5PVH model space effective interaction for M3Y and Gogny at EX=2.151MeV.

Ji	Jf	OBDM (ΔT=0)	OBDM (ΔT=1)
5/2	5/2	0.04426	0.03130
5/2	3/2	0.30436	0.21521

5/2	1/2	-0.07562	-0.05347
3/2	5/2	-0.23204	-0.16408
3/2	3/2	0.03033	0.02144
3/2	1/2	0.14802	0.10467
1/2	5/2	-0.09952	-0.07037
1/2	3/2	-0.19734	-0.13954

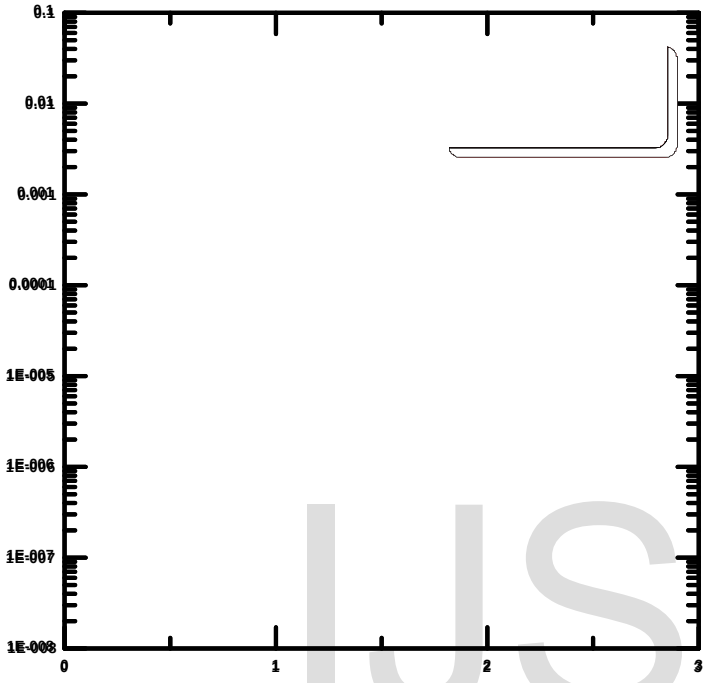

Fig. (3): Inelastic longitudinal C2 form factors for the 2_2^+2 state at Ex=2.151MeV in ^{60}Ni with a residual interaction M3Y (solid curve), the experimental data (filled circles) were taken from Ref. [18].

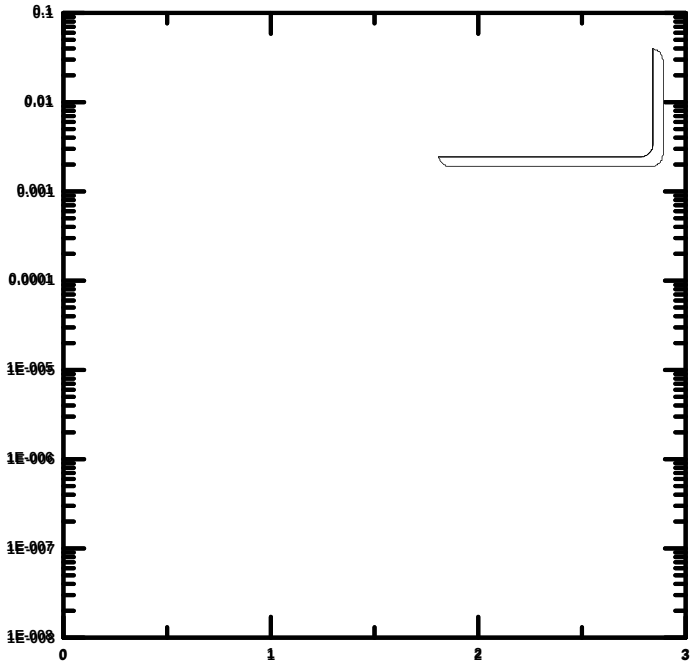

Fig. (4): Inelastic longitudinal C2 form factors for the 2_2^+2 state at Ex=2.151MeV in ^{60}Ni with a residual interaction Gogny (solid curve), the experimental data (filled circles) were taken from Ref. [18].

Figure (5) using M3Y interaction shows the calculation results for the C2 transition for third case 2_3^+ from the ground state (JπT=0+2) to the final state (JπT=2+2) at Ex=2.925 MeV, three lobes were obtained from this case, the first maximum of form factor equal to 3×10-4 at the momentum transfer region 0≤q≤0.9 fm-1, the second maximum equal to 8×10-4 at the momentum transfer 0.9≤q≤2.3 fm-1, and the third maximum is 9×10-7 at q range 2.3≤q≤3 fm-1, there is a clearly an agreement between the results and experimental data in shape and magnitude, for the first maximum, the results underestimate by 7 with respect to the form factor value, while for the second maximum, the results overestimate by 8 with respect to the form factor value.

Figure (6) using Gogny interaction shows the calculation for the C2 transition for the third case 2_3^+ from the ground state (JπT=0+2) to the final state (JπT=2+2) at Ex=2.925 MeV, three lobes were obtained from this case, the first maximum value of form factor equal to 6×10-4 at the momentum transfer region from 0 to 1 □□−1, it is very clear there is a good agreement between the theoretical and experiment data in shape and magnitude when the results underestimate by 5 with respect to the form factor value, the second maximum of form factor equal to 3×10-4 at q range 1≤q≤2.2 fm-1, which is overestimate with the experimental data by 1.5 with respect to form factor value, and the third maximum of form factor equal to 0.5×10-6 for

q range 2.3≤q≤3 fm-1. In general there is a good agreement with the experimental data.

The OBDM elements for this transitions are shown in Table (4). The experimental data are taken from Ref. [18].

Table (4): Values of the OBDM elements for the longitudinal C2 transition of the 2^+_3 2, third state of 60Ni using F5PVH model space effective interaction for M3Y and Gogny at EX=2.925 MeV.

Ji	Jf	OBDM (ΔT=0)	OBDM (ΔT=1)
5/2	5/2	-0.14391	-0.10176
5/2	3/2	-0.70889	-0.50126
5/2	1/2	-0.07401	-0.05233
3/2	5/2	0.47405	0.33521
3/2	3/2	-0.47010	-0.33241
3/2	1/2	0.19410	0.13725
1/2	5/2	-0.09000	-0.06364
1/2	3/2	-0.30114	-0.21294

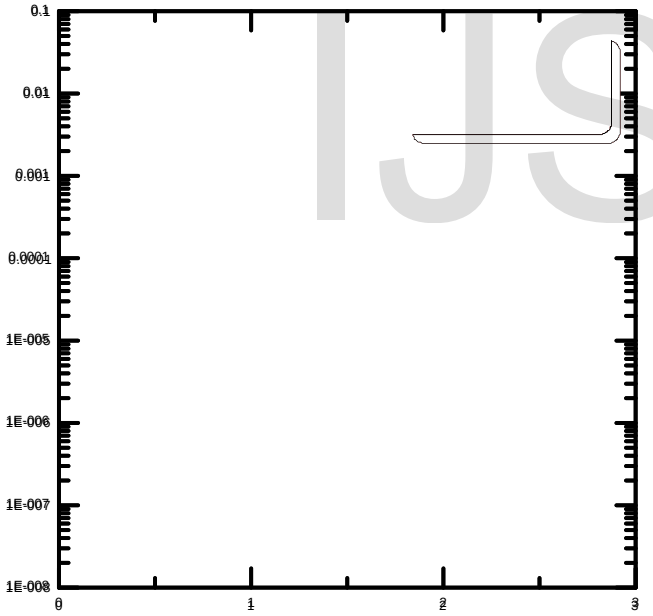

Fig. (5): Inelastic longitudinal C2 form factors for the $2^+_3 2$ state at Ex=2.925 MeV in ^{60}Ni with residual interaction M3Y(solid curve), the experimental data (filled circles) were taken from Ref. [21].

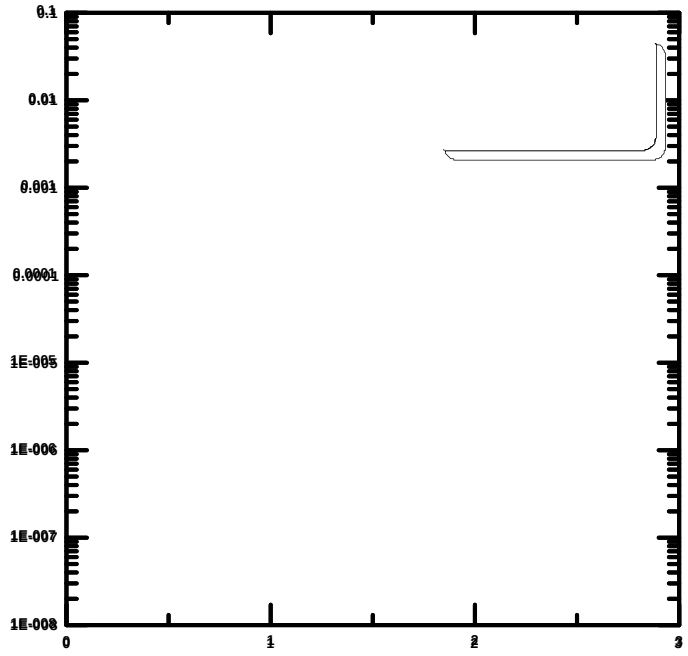

Fig. (6): Inelastic longitudinal C2 form factors for the $2^+_3 2$ state at Ex=2.925MeV in ^{60}Ni with a residual interaction Gogny (solid curve), the experimental data (filled circles) were taken from Ref. [18].

Acknowledgement: The Authors are very grateful to Prof. Dr. Raad A. Radhi for his assistance to provide the original copy of his two codes of calculation of form factors and residual interaction.

Conclusions:

From above calculations for inelastic longitudinal C2 form factors, the best one that closer the experimental data is represented by the third transition 2^+_3 using Gogny interaction.

The realistic potential M3Y, and Gogny as a residual interaction used to calculate core –polarization effects has improve the calculation, in general, the results towards the agreement with the experimental data.

The core-polarization effect enhances the form factors and makes the theoretical results of the inelastic longitudinal form factors closer to the experimental data in the C2.

The δ, σ, π and Ω mesons in M3Y interaction makes the results more real and constitute with experimental results but the density dependence of Mesons δ in spin orbit part of Gogny interaction will enhances the results very well beside the Gausse potential of central part.

References

[1] J. D. Walecka, Cambridge University Press, Cambridge, (2001) 14.

[2] R.R.Roy and B.P.Nigam, New York,John and Sons. Inc., (1967).
[3] R. Hofstadter, Annual Review of Nuclear Science, 7, (1957) 231.
[4] B. Ghosh and S. K. Sharma, Phys. Rev. C, vol. 32, p. 643, (1985).
[5] H.Uberall, New York: Academic Press, New York, (1971).
[6] M. E. Rose, USA: Technical Information Division, Oak Ridge Operations, (1948) 5.
[7] N.F.Mott, Proc. Roy, Soci. Ser, A124, (1926) 425.
[8] K. J. M. B. and R. S. Willey, Phys. Rev. Lett. 11, (1963) 518.
[9] N. Auerbach, Physical Review, 163, 4, (1967) 1203–1218.
[10] M. A. Duguay, C. K. Bockelman, T. H. Curtis, and R. A Eisenstein, 17, 1, (1966) 28.
[11] A. M. K. Y. Torizuka, Y. Kojma, M. Oyamada, K. Sugiyama, T. Terasawa, K. Itoh, A. Yamaguchi, Physical Review, 185, 4, (1969).
[12] B. Frois, S. Turck-Chieze, J. B. Bellicard, M. Huet, P. Leconte, X.-H. Phan, I. Sick, J. Heisenberg, M. Girod, K. Kumar, and B. Grammaticos, Physics Letters B, 122, 5, (1983) 347–350.
[13] R. B. M. Mooy and P. W. M. Glaudemans, Nuclear Physics A, 438, (1985) 461–481.
[14] P. K. Raina and S. K. Sharma, Phy. Rev. C, 37, 4, (1988) 1427.
[15] M. Honma, T. Otsuka, B. a. Brown, and T. Mizusaki, Physical Review C - 69,034335, (2004).
[16] O. V. Bespalova, I. N. Boboshin, V. V. Varlamov, T. a. Ermakova, B. S. Ishkhanov, a. a. Klimochkina, S. Y. Komarov, H. Koura, E. a. Romanovsky, and T. I. Spasskaya, Bulletin of the Russian Academy of Sciences: Physics, 74, 4, (2010) 542.
[17] J. M. Allmond, B. a. Brown, a. E. Stuchbery, A. Galindo-Uribarri, E. Padilla-Rodal, D. C. Radford, J. C. Batchelder, M. E. Howard, J. F. Liang, B. Manning, R. L. Varner, and C.-H. Yu, Physical Review C, 90, (2014) 1.
[18] J. M. Yao, M. Bender, and P.-H. Heenen, 1–18, (2014).
[19] unpublished, private communication.
[20] J. C. Bergestrom, I. P. Auer, M. Ahmed, F. J. Kline, J. H. Hough, H. S. Caplan, and J. L. Groh, Phys. Rev. C7, N6, (1973) 2228.
[21] R. A. Radhi, A. Bouchebak, Nucl. Phys., A716, (2003) 87.
[22] P. J. Brussard and P. W. M. Glademans, North-Holland Publishing Company, Amsterdam (1977)
[23] H. Nakada, Physical Review C 78, (2008) 1–13.
[24] B. A. Brown, Phys. Rev. C, 58, (1998) 220.